

Title: Toward elusive iodoplumbic acid HPbI₃: high-energy isochoric synthesis of hydronium forms of the PbI₃⁻ anion at elevated temperature and pressure

Authors: Szymon Sobczak^{†, a}, Athena M. Fidelli^{†, b}, Jean-Louis Do, ^b George Demopoulos*, ^c Audrey Moores*, ^b Tomislav Friščić*^b and Andrzej Katrusiak*^a

Author address: a) Department of Chemistry, Adam Mickiewicz University, Poznan; b) Department of Chemistry, McGill University; Department of Materials Engineering, McGill University

Abstract:

High-pressure and -temperature crystallization and X-ray diffraction crystallography have revealed hydronium forms of the proposed but never demonstrated iodoplumbic acid HPbI₃. Depending on the pressure range, the reaction of PbI₂ and aqueous concentrated hydriodic acid under isochoric conditions in a diamond anvil cell (DAC) held between 0.11 and 1.20 GPa produces two hydrated hydronium salts with compositions [H₃O][PbI₃] \cdot *n*H₂O (*n* = 3, 4). Comprised of polymeric one-dimensional PbI₃⁻ anions, these hydronium salts represent the so far best match for the elusive HPbI₃ progenitor of hybrid lead perovskites. We also reveal a new three-dimensional polymorph of lead iodide (PbI₂), so far known only as a layered structure.

Main text

The emergence of photovoltaic lead halide perovskites of the general formula APbI₃ (where A = alkaline metal, ammonium or organoammonium cation)¹ and composed of polymeric PbI₃⁻ anions, such as NH₄PbI₃,² [CH₃NH₃]PbI₃³⁻⁸ or CsPbI₃,⁹⁻¹¹ conducted via traditional¹² as well as unconventional methods,¹³⁻¹⁶ has inspired extensive studies on the existence of iodoplumbic(II) acid. The proposed iodoplumbic acid HPbI₃ is anticipated to be the simplest member of this class of compounds and the formally fully inorganic progenitor of hybrid as well as inorganic lead(II) perovskites. Whereas iodoplumbic acid was first proposed as a solid-state precursor for the synthesis of hybrid perovskites in 2015 by Zhao *et al.*,¹⁷ the existence of an acid with composition HPbI₃ has remained controversial.¹⁸⁻²⁵ The proposed HPbI₃ material, which results from precipitation of solutions containing PbI₂ and HI from N,N-dimethylformamide (DMF), as shown by several groups, including Kanatzidis and Hillebrecht,^{26,27} proved to be the dimethylammonium hybrid perovskite precursor [N(CH₃)₂H₂]PbI₃. Moreover, in another study Daub and Hillebrecht demonstrated that, while HPbI₃ is not accessible from the DMF solutions, the direct reaction of PbI₂ with concentrated (57% by weight) aqueous hydroiodic acid (HI) can produce two forms of hydrated iodoplumbic acids.²⁷ One exhibits the composition [H₃O]_{2x}[Pb_{1-x}I₂] \cdot (2-2x)H₂O (**1**) (*x* \approx 0.23), and is based on two-dimensional (2-D) anionic CdI₂-type sheets with approximate composition [Pb₃I₈²⁻]_{*n*}. The second one exhibits the composition (H₃O)₂Pb₃I₈ \cdot 6H₂O (**2**) (Figure 1), and is based on one-dimensional (1-D) polyanionic tapes of [Pb₃I₈²⁻]_{*n*}. Compound **2** was reported to be the first product of either crystallization of PbI₂ from concentrated aqueous HI, or of the gas-solid reaction between PbI₂ and HI vapors. Upon standing in air, **2** quickly transforms into **1**. Anions in both **1** and **2** are separated by layers of water molecules containing hydronium ions.

Overall, these prior studies indicate that an inorganic acid based on the PbI₃⁻ anion does not exist, and that the only accessible forms of iodoplumbic acid are hydronium salts of the Pb₃I₈²⁻ anion.

We now show that the crystallization of PbI_2 from concentrated aqueous HI provides, at pressure above 0.11 GPa, access to hydronium salts of 1-D polyanions with composition PbI_3^- . Based on the chemical composition of the anion, and the absence of any ammonium or metal cations, the herein reported structures are the so far closest match for the elusive HPbI_3 .

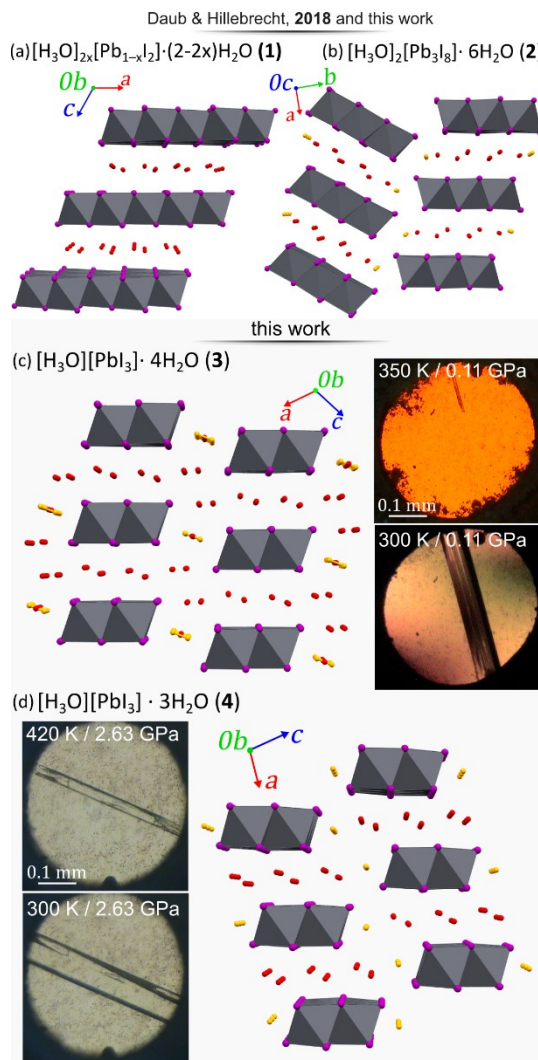


Figure 1. Four forms of hydrated iodoplumbic acid obtained in the reaction of PbI_2 with concentrated HI aqueous solution: (a) $[\text{H}_3\text{O}]_{2x}[\text{Pb}_{1-x}\text{I}_2] \cdot (2-2x)\text{H}_2\text{O}$ (compound **1**); (b) $(\text{H}_3\text{O})_2\text{Pb}_3\text{I}_8 \cdot 6\text{H}_2\text{O}$ (**2**);²⁷ and those synthesized under high p high T : (c) $(\text{H}_3\text{O})\text{PbI}_3 \cdot 4\text{H}_2\text{O}$ (**3**) and (d) $(\text{H}_3\text{O})\text{PbI}_3 \cdot 3\text{H}_2\text{O}$ (**4**). The proposed sites of H_3O^+ cations are marked in orange. Photographs show crystals **3** and **4** *in situ* grown under pressure.

With HPbI_3 apparently inaccessible by solution techniques, our study has focused on less conventional reaction environments based on introduction of mechanical energy in the form of either ball milling (mechanochemistry) or by high-pressure chemistry. Our first exploration of reactivity between PbI_2 and concentrated aqueous hydroiodic acid $\text{HI}(\text{aq})$ was done mechanochemically, by milling of the two components in the stoichiometric ratio of $\text{PbI}_2/\text{HI} = 1.5:1$ (corresponding to the 3:8 stoichiometric ratio of Pb to I, respectively). Milling produced a bright yellow powder that, upon powder X-ray diffraction (PXRD) analysis, was found to match the previously reported **1** (see ESI). Increasing the amount of $\text{HI}(\text{aq})$ for the milling stoichiometric reaction of $\text{PbI}_2/\text{HI} = 1:3$ leads to the formation of compound **2** in a pure form (see ESI). Consistent

with previous report,²⁷ upon standing in air **2** slowly transforms to **1** and, subsequently, to solid orange PbI₂. Having established that both reported hydrated iodoplumbic acids (**1** and **2**) are also accessible mechanochemically, but no new phases have been observed by milling, we turned to investigate the PbI₂/HI(aq) system under elevated pressures.

A different approach to introduce mechanical energy to a reaction system is high-pressure chemistry in a diamond anvil cell (DAC), where the application of force to the chemical-reaction system is in the form of static, hydrostatic pressure, allows for otherwise inaccessible thermodynamic coordinates.²⁸ As a reactor, the DAC represents an almost perfect closed system confining the reaction to the volume of ~0.02 mm³ between two diamond culets and a steel gasket.²⁹ The introduction of energy to the chemical reaction in the DAC is achieved by compression, typically leading to the formation of new products.³⁰ For each of the high-pressure reactions, a saturated solution of PbI₂ in HI(aq) was loaded in the DAC, and isothermally compressed. At 0.11 GPa, a polycrystalline mass precipitated that, upon subsequent recrystallization by cycles of gentle heating and cooling, led to a colorless, prism-shaped crystal suitable for structure determination by single-crystal X-ray diffraction (SCXRD). Structural analysis revealed for the crystal at 0.5 GPa a structure of formula (H₃O)PbI₃·4H₂O (**3**), comprising 1-D anionic PbI₃⁻ tapes composed of edge-sharing PbI₆-octahedra running along the crystallographic *b*-axis (Figure 1). Crystallographic parameters for **3** are distinct from those of previously reported²⁷ **1** or **2** (Figure 1, Table 1). The PbI₆-octahedra in the polyanion are slightly distorted, exhibiting four different lengths of Pb–I bonds around each metal ion: 3.046(2), 3.174(6) (twice), 3.250(6) (twice), and 3.3663(19) Å.

Table 1. Selected crystallographic data for compounds **1-4** and β-PbI₂. The structure of **1** was re-measured at ambient conditions on a crystal recovered from the DAC.

Compound	1 ^a	2 ²⁷	3	4	β-PbI ₂
<i>p</i>	0.1 MPa	0.1 MPa	0.5 GPa	2.63 GPa	2.05 GPa
<i>T</i>	300 K	300 K	300 K	300 K	320 K
Space group	<i>C2/m</i>	<i>Pbam</i>	<i>I2/m</i>	<i>P2₁/m</i>	<i>C2/m</i>
<i>a</i> (Å)	7.8946(10)	10.033(3)	16.205(2)	9.57(3)	14.06(4)
<i>b</i> (Å)	4.5598(3)	30.126(7)	4.5170(1)	4.513(3)	4.4560(12)
<i>c</i> (Å)	11.1985(18)	4.5610(10)	17.184(14)	12.98(11)	10.540(6)
β (°)	118.023(19)	-	111.50(4)	95.9(6)	93.08(12)
<i>V</i> (Å ³)	355.859	1378.66(6)	1170.3(10)	558(5)	654.9(17)
<i>D</i> _{calc} (g/cm ³)	4.638	4.290	3.666	3.883	7.013
<i>Z</i> / <i>Z'</i>	4/0.5	2/0.25	4/0.5	2/0.5	2/0.25

^aThe herein determined structure is analogous that previously reported [H₃O]_{2x}[Pb_{1-x}I₂](2-2x)H₂O (x=0.23), but with x = 0.20.

The polymeric anions are counterbalanced by hydronium cations. Although the presence of heavy atoms in **3** hinders the location of hydrogen atoms and distinguishing water molecules from H₃O⁺ cations, the latter ones are likely to form the shortest contacts with the lead-based anions. The anions are separated by tapes of hydrogen-bonded water molecules (Figure 2) O-H···O hydrogen-bonded into an extended honeycomb-like structure, O···O distances of 2.63(4) Å, 2.68(6) Å, 2.79(7) Å, periodically interrupted by short contacts with the iodoplumbate(II) anions. These

contacts are consistent with O–H···I hydrogen bonding of 3.2(2) Å, which is significantly shorter than the O···I non-bonding distance of about 3.5 Å expected from the van der Waals radii of O (1.50 Å) and I (2.04 Å) atoms.³¹ In addition to oxygen atoms in these extended hydrogen-bonded nets of water molecules, the structure of **3** also exhibits 1-D arrays of oxygen atoms that are located between pairs of PbI₃[−] anions (Figure 2b). The anionic framework of **3** is analogous to that in NH₄CdCl₃,³² NH₄PbI₃,³³ CsPbI₃³⁴ and RbPbI₃.^{35,36} Consequently, **3** can be seen as the acidic, hydronium-based analogue of these perovskite solids.

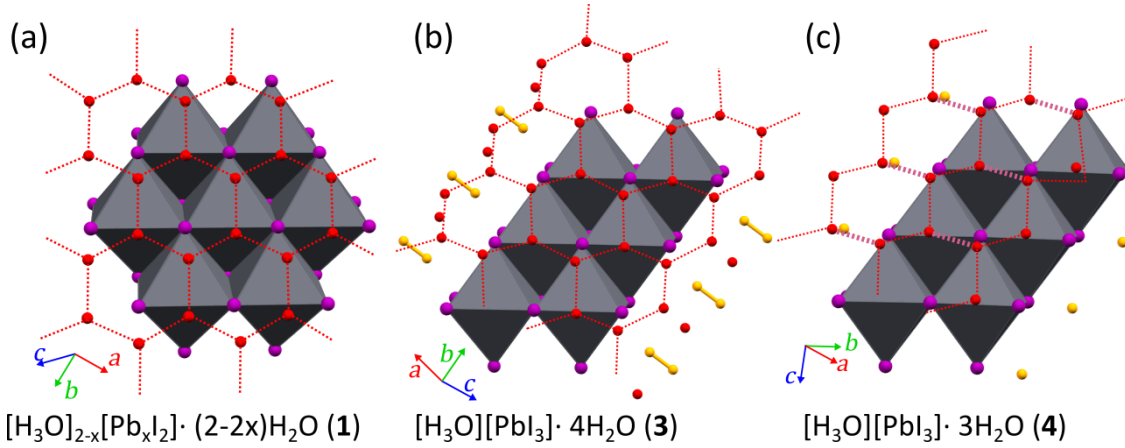


Figure 2. Crystal structures of (a) **1**; (b) **3**; and (c) **4** viewed perpendicular to the honeycomb water networks, with the longer O···O distances shown lighter. The oxygen atom sites suggested for H₃O⁺ ions are shown in orange.

While increasing the pressure up to 1.20 GPa does not affect the crystals of **3**, releasing the pressure to 0.1 MPa quickly leads to their transformation into **1** (Figure 3). The transformation takes place in a single-crystal-to-single-crystal (SCSC) manner, as shown by X-ray diffraction on the crystal recovered from the DAC (see ESI), which revealed a clear matrix relationship between the lattices for the starting crystal of H₃OPbI₃·4H₂O (**3**) and the daughter phase **1**:

$$\begin{pmatrix} -1/3 & 0 & 1/3 \\ 0 & -1 & 0 \\ 2/3 & 0 & 1/3 \end{pmatrix} \begin{pmatrix} a_3 \\ b_3 \\ c_3 \end{pmatrix} = \begin{pmatrix} a_1 \\ b_1 \\ c_1 \end{pmatrix},$$

where a_1, b_1, c_1 and a_3, b_3, c_3 are sets of unit-cell parameters for **1** and **3**, respectively (Table 1).

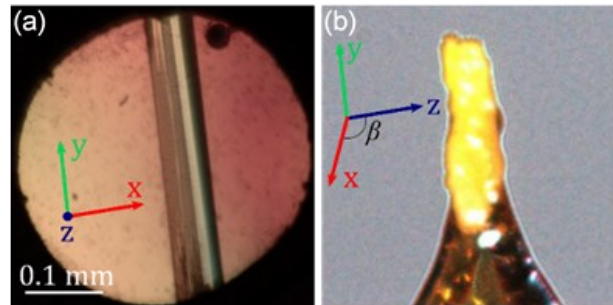


Figure 3. A crystal of **3**: as grown in the DAC (a) and (b) then recovered to ambient conditions and transformed to **1**, on a nylon loop. Crystal axes are indicated.

The quality of the crystal recovered to 0.1 MPa permitted the SCXRD measurement of lattice dimensions and structure refinement, which revealed monoclinic symmetry (Table 1, also SI). It is highly pseudo-symmetric (see the SI) and similar to the trigonal structure previously reported for **1**.²⁷ The two determinations of this layered structure of $[\text{H}_3\text{O}]_{2x}[\text{Pb}_{1-x}\text{I}_2] \cdot (2-2x)\text{H}_2\text{O}$ are consistent, except for somewhat lower x value resulting from our SCXRD measurement (0.20 compared to 0.23). The difference, we believe, indicates the possibility of **1** to adopt a wide range of compositions. The highly topotactic transformation from **3** to **1** requires a transition from 1-D to 2-D polyanions, in which some of the water and HI molecules leave the structure, probably by diffusion, while the edge-sharing connectivity of PbI_6 -octahedra is preserved in both materials.

Above 1.2 GPa and at temperature above 420 K, we obtained a pink-colored crystalline material (Figure 4a), different from **3**. Subsequent SCXRD was conducted at 320 K and above 2.05 GPa, revealing a high-pressure polymorph of PbI_2 , herein termed β - PbI_2 . The β - PbI_2 displays a reverse solubility, as we observed the growth of β - PbI_2 crystals on increasing the temperature, and their dissolution on cooling of the DAC. This new form of β - PbI_2 crystallizes in the monoclinic space group $C2/m$ with unit-cell parameters $a = 14.10(3)$ Å, $b = 4.4548(9)$ Å, $c = 10.610(5)$ Å, and $\beta = 92.89(11)^\circ$, and it has a 3-D framework of alternating six- and seven- coordinated Pb^{2+} cations bridged by iodide ions (Table 1, Figure 4d,e, also see ESI). In this respect, it contrasts with the well-known 2-D layered structure with six-coordinated Pb^{2+} cations in α - PbI_2 . To the best of our knowledge, this is the first observation of polymorphism in PbI_2 . The formation of β - PbI_2 is consistent with higher pressure leading to increased coordination numbers due to stronger compression of anions than cations.³⁷

We obtained a yet another crystalline phase by two different methods, either by recrystallizing **3** above 1.2 GPa or by a spontaneous recrystallization of β - PbI_2 crystals in the DAC below 350 K (Fig 3a-c). Below 1.2 GPa, at 320 K, pink β - PbI_2 dissolves and colorless needle-like crystals of another new phase (**4**) appear. Recrystallization by mild temperature oscillation produced a diffraction-quality single crystal of **4**, revealing another structure based on PbI_3^- polyanions (Table 1). Compound **4** was found to exhibit the formula $(\text{H}_3\text{O})\text{PbI}_3 \cdot 3\text{H}_2\text{O}$, based on identical polymeric anions with edge-sharing PbI_6 -octahedra, as those in **3**, but with a lower content of water of crystallization (Figure 3). The lower content of water in **4** compared to **3** is consistent with shorter $\text{I} \cdots \text{I}$ contacts at higher pressure. In this case also, four distinct lengths of $\text{Pb}-\text{I}$ bonds are present in the anions: 2.81(4), 3.186(12) (twice), 3.232(11) (twice), and 3.34(4) Å. In **4**, oxygen atoms of water molecules form ribbons (about 10 Å wide). Within the ribbons shorter hydrogen bonds [$\text{O} \cdots \text{O}$ distances of 2.73(9) Å] are arranged into three 1-D zigzag chains, interconnected by weaker bonds [$\text{O} \cdots \text{O}$ distance of 3.1(2) Å] into a strongly distorted honeycomb motif. The ribbons separate the adjacent pairs of PbI_3^- polyanions. Additionally, there are also oxygen atoms not involved in any $\text{O} \cdots \text{O}$ contacts commensurate with hydrogen bonds, but they are each close to three iodine atoms of PbI_3^- anions, with $\text{O} \cdots \text{I}$ distances of 3.187(12) (twice), 3.232(11) (twice), 2.80(4) (once) and 3.33(4) (once) Å at (at 2.63 GPa, 300 K). According to the criterion of close vicinity to the anions, it is tempting to identify these oxygen atoms as belonging to hydronium species, although the location of protons by X-ray diffraction currently is not possible.

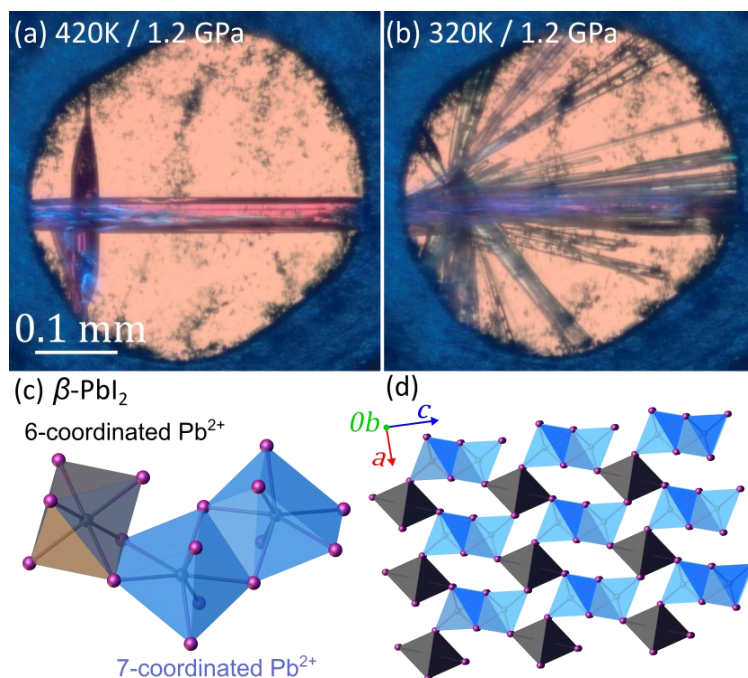


Figure 4. Pink single crystals of β -PbI₂ at 1.2 GPa and: (a) 420K and (b) 320 K covered by a bundle of needle crystals of **3**. Views of the β -PbI₂ structure: (c) six- and seven-coordinated Pb²⁺ cations and (d) the 3-dimensional network viewed along the crystallographic *b*-axis.

The appearance of the herein described series of structures comprising the α - and β -forms of PbI₂, as well as iodoplumbic acids **1** – **4** can be rationalized through the interplay of intercalation of HI(aq) and high pressure on the α -PbI₂ structure. The observation of different structures at different conditions outlines several stability regions in the preference *p-T* diagram (Figure 5), where the low-pressure end-member is α -PbI₂ with a 2-D layer structure, and the high-pressure end-member is β -PbI₂, in which some of the Pb²⁺ cations become 7-coordinated to form a 3-D network.

All members of the series, exhibiting either 1-D, 2-D or 3-D structures, contain the common motif of edge-sharing PbI₆-octahedra (Figs. 1 and 2), based on Pb–I bonds that are by far and large the least compressed elements constituting the scaffolds of the structures (Table 1). In contrast, the I⋯I contacts between PbI₂ sheets or the iodoplumbate(II) anions are expected to be considerably weaker and most likely to be affected by pressure, temperature and overall chemical environment. The iodoplumbic acid structures **1** – **4** can be seen as resulting from the α -PbI₂ structure transformed through the intercalation of water and hydronium ions from HI(aq), resulting in the water- and hydronium-mediated OH⋯I^{δ-} bonds between anionic sheets and tapes, which prevents their contacts involving electronegative iodine atoms.

The observation of compounds **1-3** at pressures up to 1.2 GPa is explained by progressive intercalation of ions from HI(aq) into the PbI₂ structure, leading to a PbI₃⁻ anion composition. At 1.2 GPa a partial desorption of water is observed, resulting in compound **4** that maintains the PbI₃⁻ anions. It is consistent with our previous general observation that pressures above 1 GPa often destabilize hydrates.^{38,39} Ultimately, exposing the system to still higher pressure and temperature completely prevents intercalation and leads to formation of a 3-D structure through creation of new Pb–I bonds and 7-coordinated lead(II) ions.

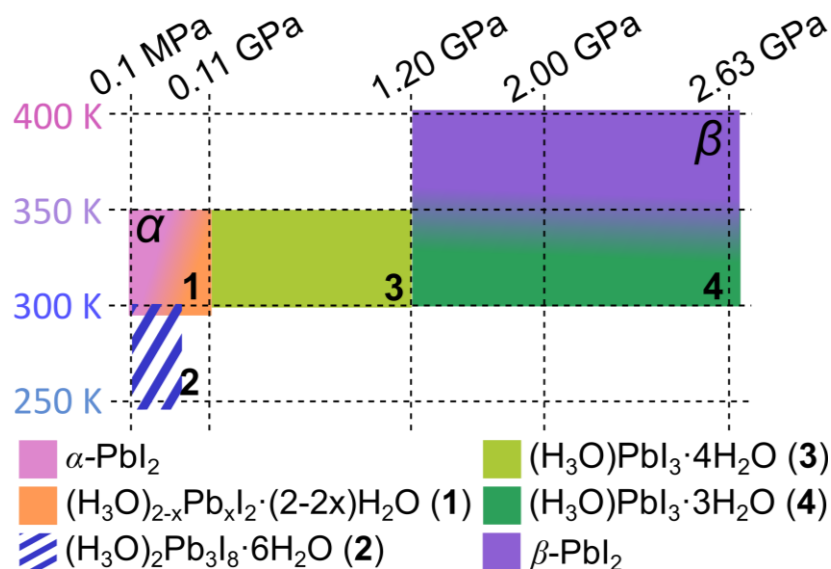


Figure 5. The p/T preference diagram of PbI_2 and $\text{HI}(\text{aq})$ system, with their end members of 2D-polymorph $\alpha\text{-PbI}_2$ and 3D-polymorph $\beta\text{-PbI}_2$. Iodoplumbic acids **1** and **2** are obtained by milling and vapor reactions, whereas **1**, **3**, **4** and $\beta\text{-PbI}_2$ were obtained by high-pressure synthesis in the DAC.

In summary, high-energy isochoric syntheses in a DAC revealed the existence of two new hydrated iodoplumbic acid solids, based on one-dimensional polyanions of composition PbI_3^- . The anion composition makes the herein observed high-pressure hydronium salts the so far best match to the elusive iodoplumbic acid HPbI_3 , which is of fundamental importance as the progenitor of the highly popular class of hybrid perovskite materials. We have suggested a mechanism for the formation of iodoplumbic acids, based on the intercalation of water and hydronium ions through $\text{OH}\cdots\text{I}^\delta-$ and $\text{OH}^+\cdots\text{I}^\delta-$ hydrogen bonds that prevent close contacts between $\text{I}^\delta-$ atoms. The presence of four such compounds (**1-4**) in the pressure region up to 2.63 GPa is consistent with the high sensitivity of the system to the external stimuli.

High-energy crystallization in the DAC also gave rise to the so far first known polymorph of $\beta\text{-PbI}_2$ which, unlike the commonly known form based on 2-dimensional sheets, presents an unprecedented PbI_2 structure based on Pb-I polyhedra connected into a three-dimensional structure. This work highlights the potential of crystallization from the high-energy DAC environment as a simple and straightforward means to discover new phases, even in systems that have been extensively studied, over a long time. The herein observed hydrated iodoplumbic acids and a new form of PbI_2 , together with previously reported structures, represent a closely related family of structures, in which the electrostatic repulsion between electronegative atoms is reduced by the intercalation of water molecules and hydronium cations, and is overcome completely at high pressure (>2 GPa) and temperature ($>350\text{K}$), when a new polymorph $\beta\text{-PbI}_2$ appears.

Acknowledgments

We acknowledge the McGill Sustainability Systems Initiative (MSSI) and NSERC Discovery Grant program. S.S. is grateful to the grant POWR.03.02.00-00-I023/17 co-financed by the European Union through the European Social Fund under the Operational Program Knowledge Education Development.

References

1. Y. Zheng, H. Sato, P. Wu, H. J. Jeon, R. Matsuda, S. Kitagawa, *Nat. Commun.* **2017**, *8*, 100.
2. L.-Q. Fan, J.-H. Wu, *Acta Crystallogr.* **2007**, E63, i189–i189.
3. J. Burschka, N. Pellet, S. J. Moon, R. Humphry-Baker, P. Gao, M. K. Nazeeruddin, M. Grätzel, *Nature* **2013**, *499*, 316–319.
4. N. J. Jeon, J. H. Noh, Y. C. Kim, W. S. Yang, S. Ryu, S. Il Seok, *Nat. Mater.* **2014**, *13*, 897–903.
5. H. Z. Sheng Huang, Peng Huang, Lei Wang, Junbo Han, Yu Chen, *Adv. Mater.* **2019**, *31*, 1903830.
6. M. Szafranski, A. Katrusiak, *J. Phys. Chem. Lett.* **2016**, *7*, 3458–3466.
7. M. Szafranski, A. Katrusiak, *J. Phys. Chem. Lett.* **2017**, *8*, 2496–2506.
8. M. Shirayama, H. Kadowaki, T. Miyadera, T. Sugita, M. Tamakoshi, M. Kato, T. Fujiseki, D. Murata, S. Hara, T. N. Murakami, S. Fujimoto, M. Chikamatsu, H. Fujiwara, *Phys. Rev. Appl.* **2016**, *5*, 1–25.
9. D. Prochowicz, R. Runjhun, M. M. Tavakoli, P. Yadav, M. Sasaki, A. Q. Alanazi, D. J. Kubicki, Z. Kaszkur, S. M. Zakeeruddin, J. Lewiński, M. Grätzel, *Chem. Mater.* **2019**, *31*, 1620–1627.
10. Y. Wang, M. Ibrahim Dar, L. K. Ono, T. Zhang, M. Kan, Y. Li, L. Zhang, X. Wang, Y. Yang, X. Gao, Y. Qi, M. Grätzel, Y. Zhao, *Science*, **2019**, *365*, 591–595.
11. W. Ahmad, J. Khan, G. Niu, J. Tang, *Sol. RRL* **2017**, *1*, 1–9.
12. T. Baikie, Y. Fang, J. M. Kadro, M. Schreyer, F. Wei, S. G. Mhaisalkar, M. Grätzel, T. J. White, *J. Mater. Chem. A* **2013**, *1*, 5628–5641.
13. D. Prochowicz, M. Franckevičius, A. M. Cieślak, S. M. Zakeeruddin, M. Grätzel, J. Lewiński, *J. Mater. Chem. A* **2015**, *3*, 20772–20777.
14. D. Prochowicz, P. Yadav, M. Saliba, M. Sasaki, S. M. Zakeeruddin, J. Lewiński, M. Grätzel, *Sustain. Energy Fuels* **2017**, *1*, 689–693.
15. W. Huang, J. S. Manser, S. Sadhu, P. V. Kamat, S. Ptasińska, *J. Phys. Chem. Lett.* **2016**, *7*, 5068–5073.
16. Y. Zong, Y. Zhou, M. Ju, H. F. Garces, A. R. Krause, F. Ji, G. Cui, X. C. Zeng, N. P. Padture, S. Pang, *Angew. Chem. Int. Ed.* **2016**, *55*, 14723–14727.
17. F. Wang, H. Yu, H. Xu, N. Zhao, *Adv. Funct. Mater.* **2015**, *25*, 1120–1126.
18. S. Pang, Y. Zhou, Z. Wang, M. Yang, A. R. Krause, Z. Zhou, K. Zhu, N. P. Padture, G. Cui, *J. Am. Chem. Soc.* **2016**, *138*, 750–753.
19. Z. Zhou, S. Pang, F. Ji, B. Zhang, G. Cui, *Chem. Commun.* **2016**, *52*, 3828–3831.
20. M. Long, T. Zhang, Y. Chai, C. F. Ng, T. C. W. Mak, J. Xu, K. Yan, *Nat. Commun.* **2016**, *7*, 1–11.
21. M. Long, T. Zhang, H. Zhu, G. Li, F. Wang, W. Guo, Y. Chai, W. Chen, Q. Li, K. S. Wong, J. Xu, K. Yan, *Nano Energy* **2017**, *33*, 485–496.
22. F. Ji, S. Pang, L. Zhang, Y. Zong, G. Cui, N. P. Padture, Y. Zhou, *ACS Energy Lett.* **2017**, *2*, 2727–2733.
23. Y. Wei, W. Li, S. Xiang, J. Liu, H. Liu, L. Zhu, H. Chen, *Sol. Energy* **2018**, *174*, 139–148.
24. X. Ding, H. Chen, Y. Wu, S. Ma, S. Dai, S. Yang, J. Zhu, *J. Mater. Chem. A* **2018**, *6*, 18258–18266.
25. Z. Liu, L. Qiu, E. J. Juarez-Perez, Z. Hawash, T. Kim, Y. Jiang, Z. Wu, S. R. Raga, L. K. Ono, S. (Frank) Liu, Y. Qi, *Nat. Commun.* **2018**, *9*, 1–11.
26. W. Ke, I. Spanopoulos, C. C. Stoumpos, M. G. Kanatzidis, *Nat. Commun.* **2018**, *9*:4785.

27. M. Daub, H. Hillebrecht, *Zeit. Anorg. Allg. Chemie* **2018**, *644*, 1393–1400.
28. A. Katrusiak, *Acta Cryst.* **2019**, *B75*, 918–926.
29. A. Katrusiak, in *Int. Tables Crystallogr.* (2019). *Vol. H.*, 2019, pp. 156–173.
30. S. Sobczak, A. Katrusiak, *Inorg. Chem.* **2019**, *58*, 11773–11781.
31. S. Alvarez, *Dalton Trans.* **2013**, *42*, 8617–8636.
32. H. Brasseur, L. Pauling, *J. Am. Chem. Soc.* **1938**, *60*, 2886–2890.
33. D. Bedlivy, K. Mereiter, *Acta Cryst.* **1980**, *B36*, 782–785.
34. C. K. Møller, *Nature* **1958**, *182*, 1436–1436.
35. H. J. Haupt, F. Huber, C. Krüger, H. Preut, D. Thierbach, *Zeit. Anorg. Allg. Chemie* **1977**, *436*, 229–236.
36. D. M. Trots, S. V. Myagkota, *J. Phys. Chem. Solids* **2008**, *69*, 2520–2526.
37. A. Pórolniczak, S. Sobczak, A. Katrusiak, *Inorg. Chem.* **2018**, *57*, 8942–8950.
38. H. Tomkowiak, A. Olejniczak, A. Katrusiak, *Cryst. Growth Des.* **2013**, *13*, 121–125.
39. F. Safari, A. Olejniczak, A. Katrusiak, *Cryst. Growth Des.* **2020**, *20*, 3112–3118.